LETTERS

A belt of moonlets in Saturn's A ring

Miodrag Sremčević[1], Jürgen Schmidt[2], Heikki Salo[3], Martin Seiß[2], Frank Spahn[2] & Nicole Albers[1]

The origin and evolution of planetary rings is one of the prominent unsolved problems of planetary sciences, with direct implications for planet-forming processes in pre-planetary disks[1]. The recent detection of four propeller-shaped features in Saturn's A ring[2] proved the presence of large boulder-sized moonlets in the rings[3–5]. Their existence favours ring creation in a catastrophic disruption of an icy satellite rather than a co-genetic origin with Saturn, because bodies of this size are unlikely to have accreted inside the rings. Here we report the detection of eight new propeller features in an image sequence that covers the complete A ring, indicating embedded moonlets with radii between 30 m and 70 m. We show that the moonlets found are concentrated in a narrow 3,000-km-wide annulus 130,000 km from Saturn. Compared to the main population of ring particles[6–8] (radius $s < 10$ m), such embedded moonlets have a short lifetime[9] with respect to meteoroid impacts. Therefore, they are probably the remnants of a shattered ring-moon of Pan size or larger[2], locally contributing new material to the older ring. This supports the theory of catastrophic ring creation in a collisional cascade[9–12].

On 20 August 2005 the Cassini spacecraft recorded an occultation of the star α Scorpii (α Sco, Antares) by Saturn's rings. The Imaging Science Subsystem (ISS)[13] Narrow Angle Camera (NAC) took 26 images with a complete radial coverage of Saturn's A ring. Four of these images show seven propeller features, all radially inward from the Encke division, which is also where the first propellers were detected[2] in images obtained during the Saturn Orbit Insertion (SOI) manoeuvre of Cassini. Shortly after the α Sco sequence, NAC recorded 105 images of the Encke gap. In this 'movie' sequence, one additional propeller is found 340 km outside the Encke division. Altogether we can identify eight new moonlet-induced structures (see Supplementary Information for details; Figs 1, 2 and Supplementary Figs 1–9); of these eight, five re-occur in subsequent images, confirming their orbital motion (Fig. 1).

All propellers were identified in images of the backlit rings, so that dark features could correspond either to very dense regions (totally blocking the light) or to mostly empty regions (not scattering any light). Similarly, the bright propeller streaks could be either density depletions or density enhancements. Our photometric modelling of simulated embedded moonlets and ring background (Supplementary Figs 12–14) strongly favours the correspondence of bright parts of the propeller with increased density. Taking into account the unresolved self-gravity wakes in ring A[14–16], which reduce the brightness compared to a uniform ring[2,17], we can account qualitatively for the ring background I/F (where I is brightness and F is the solar flux) for α Sco and SOI image geometries (Supplementary Fig. 12). However, it is still a challenge to explain quantitatively the large brightness difference between the propellers and the background. A potential factor contributing to propeller brightness could be the release of debris from regolith-covered ring particles[18,19] in the moonlet-perturbed region, where the relative impact speeds of particles are considerably larger than in the background ring. Our models (Supplementary Figs 13 and 14) imply that this debris can significantly enhance the brightness of the moonlet-induced wakes—the waves induced in the ring downstream from the moonlet by its gravity[20,21]—which we suggest are seen in images as propellers.

We can determine the propeller dimensions by fitting the brightness I/F of the wings to a double-gaussian function (Fig. 2 and Supplementary Information). The observed (Fig. 3) azimuthal (W) and radial (h) sizes rule out the cubic scaling $W \propto h^3$ predicted theoretically[4,5,22] for the length of an incomplete gap opened by a moonlet. Instead, a nearly linear relationship $W \propto h^{\beta}$, where $\beta \approx 1-1.5$, is indicated.

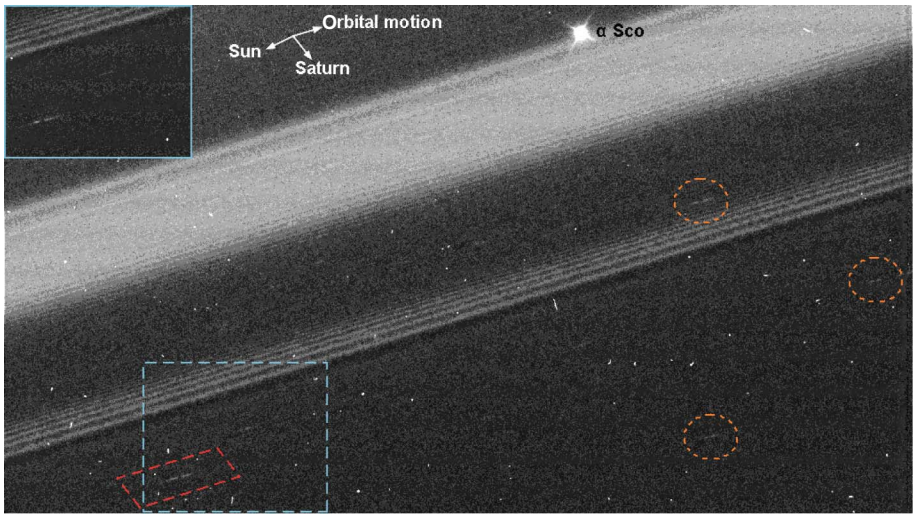

Figure 1 | Four new propellers in Saturn's A ring seen by Cassini. Part of the image N1503229987 (Supplementary Figs 1 and 2) with four propellers (enclosed in different colours to facilitate comparison). The greyscale colour represents I/F in the range of 0.0071–0.0167. The inset demonstrates the re-occurrence of the largest propeller (blue dashed rectangle) in the image N1503230047 (orbital motion is subtracted; Supplementary Figs 1 and 3). The images are 2 of 26 in the α Sco sequence with a complete radial coverage of the A ring and part of the Cassini division. In this sequence, NAC observed the unlit side of the rings, with a phase angle of 126° and incidence and emission angles of 111° and 58°, respectively. The images were taken at 60 s intervals with 50 ms exposure in a clear filter with a resolution of 1 km per pixel in the radial direction and 0.5 km per pixel in the azimuthal direction that is only superseded by the SOI image sequence[2,13].

[1]Laboratory for Atmospheric and Space Physics, University of Colorado at Boulder, 392 UCB, Boulder, Colorado 80309-0392, USA. [2]Nonlinear Dynamics, Department of Physics, University of Potsdam, Am Neuen Palais 10, 14469 Potsdam, Germany. [3]Astronomy Division, Department of Physical Sciences, University of Oulu, 90014 Oulu, Finland.

A nearly linear scaling is expected for the size of the wake region, because wakes are damped (independently of the moonlet size) after a certain number of wake crests[20,22,23] (see Supplementary Information). This supports our interpretation that the bright streaks seen in images are actually related to moonlet wakes. A deviation from the linear trend follows naturally if the propeller brightness is further enhanced by release of regolith debris in the wake region (Fig. 3).

All propellers in the α Sco and SOI images are found in an annulus between 128,700 and 131,700 km from Saturn. A homogeneous distribution of moonlets over the whole A ring is extremely unlikely with the given observation (a probability of 10^{-6} from poissonian statistics applied to the α Sco image sequence). One propeller-moon orbits at a saturnian distance of 134,000 km outside the Encke division (Fig. 2b). Thus, moonlets are found preferentially inward from the Encke division, and are significantly less frequent elsewhere in the A ring. The moonlet sizes are estimated from the propeller dimensions, and range from 30 to 70 m in radius (Fig. 4). Identifying the brightness enhancements in images as moonlet wakes, we re-interpret the SOI sequence moonlet radii to be about 20 m.

The resulting cumulative moonlet size distribution (Fig. 4) shows a steep slope of index $Q = 10$, the fairly large error bars requiring a minimal slope of $Q > 8$. The non-discovery of propellers in the α Sco images of the rest of the A ring implies a very low frequency there or locally, even the total absence of objects larger than 10 m. Moreover, from the size distribution we expect no moonlets larger than about 350 to 500 m in the moonlet region, which is consistent with the non-detection of circumferential gaps[5] apart from the Keeler and Encke gaps. It is also possible that Pan and Daphnis, together with putative non-detected larger moonlets in the Encke gap[13], form a shallower wing of the size distribution[24].

The inhomogeneous distribution of moonlets in the A ring and their rather steep size distribution have interesting consequences for the formation and evolution of Saturn's rings. It has been suggested that the embedded moonlets favour a scenario of ring creation in a break-up of a larger body[2]. However, it seems unlikely that moonlets are remainders of a single catastrophic event that created the whole ring system, because in this case a uniform distribution would emerge. Instead, the moonlet belt is compatible with a more recent break-up of a body orbiting in the A ring. Accretion of moonlets from a population of smaller ring particles seems equally unlikely: even if the absence of accretion radially inward from a radial distance of 128,000 km from Saturn could be attributed to the increasing tidal forces nearer to the planet[25], it would be difficult to understand why no moonlets accreted in the outer A ring. The probability of finding coincidentally no propellers outside 132,000 km in the α Sco images, if moonlets were uniformly distributed, is still less than 5×10^{-4}. Furthermore, the fact that one propeller resides in the Prometheus 12:11 density-wave-train and another in the Pan-induced wakes (Fig. 1 and Fig. 2b) demonstrates that propellers are not necessarily destroyed in perturbed ring regions. Hence, the possibility that the outer A ring is too perturbed to harbour such moonlets also seems unlikely.

Catastrophic collisions are a common concept in the theory of ring evolution, and shattering of larger moons in a collisional cascade has been proposed[9–12]. In this scenario the disruption of larger fragments at a later time gradually adds fresh material to the existing ring system. Evidence for a very recent (1984) disrupting impact of a metre-sized object on an icy boulder of similar size in Saturn's D ring is given by the detection of a rapidly evolving tightly wound spiral pattern[26]. Moreover, a number of potential target moons of kilometre size still exist at present in the rings (Pan, Daphnis, Atlas), and smaller moons are expected in the gaps[13]. Consequently, we may expect to

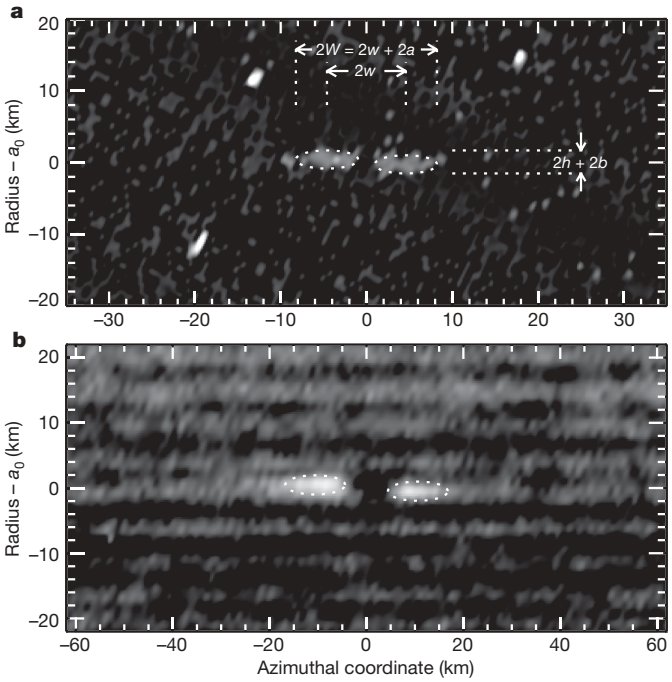

Figure 2 | Close-up view and re-projection of two propeller structures. **a**, The red rectangle from Fig. 1; **b**, the portion of the image N1503243458 (image in Encke gap 'movie' sequence covering 44° of the circumference with resolution better than 2 km per pixel; first-order Pan wakes are visible in the background, Supplementary Fig. 6). Structural fits are indicated: $2W = 2w + 2a$ is the total azimuthal extent and $2h$ is the radial separation of the propeller wings (corresponds to Δr in ref. 2), whereas (a, b) denote the semi-major axes of ellipses fitted to the wings (dots). In **a**, $a_0 = 131{,}525$ km; in **b**, $a_0 = 134{,}079$ km. Orbital motion is to the right.

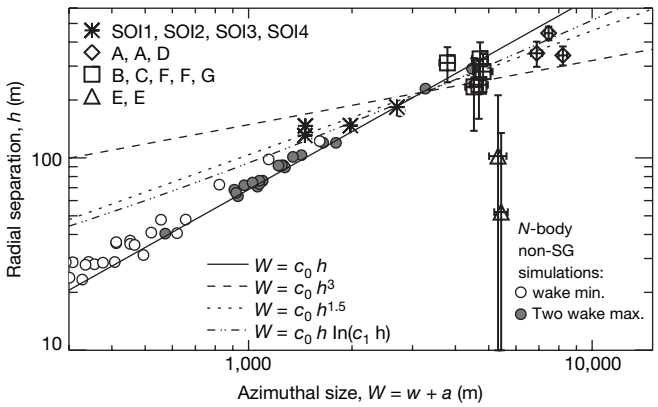

Figure 3 | Nearly linear spatial scaling of the features points to moonlet wakes. Shown is the radial separation h of the propeller wings as a function of their azimuthal extent $W = w + a$. Asterisks represent propellers in SOI images[2]; symbols with $\pm 1\sigma$ error bars (A–E, Supplementary Table 2) denote seven new propellers from the α Sco sequence. Various fits to the data are indicated, excluding the anomalous points E; the cubic relation $W \propto h^{\beta}$ where $\beta = 3$ is clearly ruled out by the data, which seem to suggest $\beta \approx 1 - 1.5$. This nearly linear scaling implies that propellers are related to the moonlet wakes, whose azimuthal wavelength $\lambda_1 = 3\pi h$ increases linearly with radial distance $h = |r - a_0|$ to the moonlet. A linear scaling $W \propto \lambda_1 \propto h$ would be obtained if the wakes are damped after a certain number of wake-crests, independently of the moon size. Such an enhanced localized damping is indeed expected near the point of streamline crossing[20], roughly two wake cycles downstream from the moon, which is confirmed by N-body simulations[22,23] (Supplementary Fig. 10; here we plot results from non-self-gravitating (non-SG) simulations). The excess to the linear scaling is also in accordance with the picture that the visibility of propellers is partly caused by release of debris in high-speed impacts in the region of moonlet-induced wakes. Namely, with increased moonlet size, enhanced debris production per surface area is expected. Let us assume an exponential downstream decay of the optical depth of debris caused by re-accumulation. Then, a critical minimum optical depth of debris is required for the propeller to stand out against the background, leading to a logarithmic dependence between azimuthal extent and debris release rate. Furthermore, assuming that debris production scales as some power of moonlet mass suggests $W \propto h \ln(c_1 h)$.

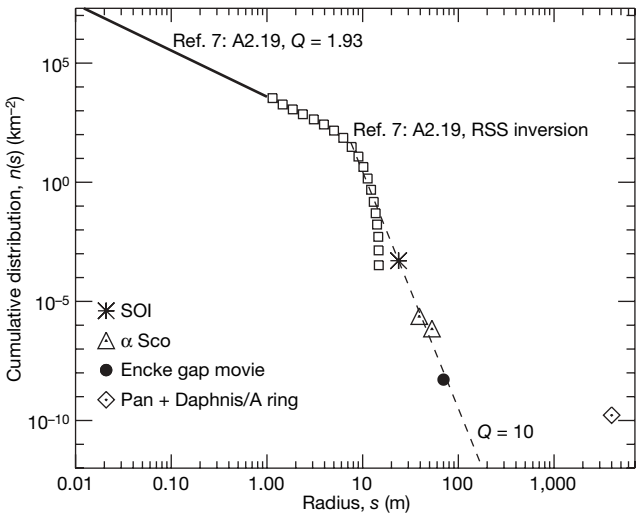

Figure 4 | Cumulative size distribution of particles in the moonlet belt region. The Voyager Radio Science Subsystem (RSS) results[7] have a knee around $s = 10$ m, indicating a steeper slope for $s > 10$ m, the latter points having an order of magnitude uncertainty (A2.19 refers to the A-ring region studied by RSS). Individual moonlet sizes are derived from the spatial scaling of the propellers. The largest density enhancement in a moonlet wake lies at a radial distance[5,22,30] $h/H \approx 4.5 \pm 0.5$, where $H = a_0[M/(3M_{\mathrm{Saturn}})]^{1/3}$ is the moonlet's Hill scale, which is proportional to its radius. M denotes moonlet mass and M_{Saturn} denotes Saturn's mass. Assuming densities between 0.5 and 0.9 g cm^{-3}, we may estimate the moonlet radius as $s = 0.14h$ with a probable error of about 15% from the radial separation of the propeller wings. Assuming the whole A ring as basis for calculation (instead of only the moonlet belt within $r_1 = 128{,}500$ km and $r_2 = 134{,}500$ km) would decrease α Sco values by a factor of three, and, likewise, a narrower moonlet belt would increase α Sco values by a factor of two at most. Other points are affected even less. Additionally, poissonian statistics of propeller appearances in the images implies a statistical error of 50% for SOI, <50% for α Sco and 100% for the Encke movie sequence. The latter point has additional uncertainty owing to long image exposure (2 s) and possible smear, which might hide propellers of similar size. However, all these factors are small and do not change the overall picture nor the inferred steepness of the distribution. Note that identifying bright features as gaps would just imply systematically two-times larger sizes s, not affecting the overall conclusions.

find traces of the past break-up of larger objects in the current rings[12]. Steep size-slopes between $Q = 5$ and $Q = 8$ have been reported for the fragments of giant impacts[24,27]. Combining all moonlets ($s > 15$ m) in the belt, we obtain a sphere of roughly 10 km in radius, suggesting that a moon of Pan size or larger has been shattered. With a mean ejection speed of 50 m s^{-1} the debris is spread over a radial width of 3,000 km (see Supplementary Information). Using a ring viscosity[28] of $\nu = 90$ cm^2 s^{-1} and a belt width $\Delta r = 3{,}000$ km, we obtain a characteristic time $t_{\mathrm{visc}} = (\Delta r)^2/\nu$ of 3×10^7 years, which should give an upper limit for closing the gap previously kept open by the moon. The debris evolves by further shattering resulting from meteoroid bombardment. Whereas larger fragments are gradually ground down to smaller sizes, their size-slope steepening with time, the distribution of ring particles smaller than about 10 m is stabilized by a balance between aggregation and disintegration[18,19]. We estimate the time for the destruction of all moonlets (see Supplementary Information) larger than 100 m in the belt to be 10^8 years (threefold for moonlets >50 m), although the uncertainties of the model[9,29] imply large errors. Thus, the inferred steepness of the moonlets' size distribution and their apparent depletion in the rest of the A ring represent different phases of the process of moonlet destruction, like a clock displaying the age of a ring region.

Note added in proof: Another study of A-ring propellers using a larger set of Cassini data has been recently submitted to *The Astronomical Journal*[31].

Received 21 May; accepted 30 August 2007.

1. Burns, J. A. & Cuzzi, J. N. Our local astrophysical laboratory. *Science* **312,** 1753–1755 (2006).
2. Tiscareno, M. S. *et al.* 100-metre-diameter moonlets in Saturn's A ring from observations of propeller structures. *Nature* **440,** 648–650 (2006).
3. Julian, W. H. & Toomre, A. Non-axisymmetric responses of differentially rotating disks of stars. *Astrophys. J.* **146,** 810–830 (1966).
4. Spahn, F. & Sremčević, M. Density patterns induced by small moonlets in Saturn's rings? *Astron. Astrophys.* **358,** 368–372 (2000).
5. Sremčević, M., Spahn, F. & Duschl, W. J. Density structures in perturbed thin cold discs. *Mon. Not. R. Astron. Soc.* **337,** 1139–1152 (2002).
6. Marouf, E. A., Tyler, G. L., Zebker, H. A., Simpson, R. A. & Eshleman, V. R. Particle size distributions in Saturn's rings from Voyager 1 radio occultation. *Icarus* **54,** 189–211 (1983).
7. Zebker, H. A., Marouf, E. A. & Tyler, G. L. Saturn's rings — particle size distributions for thin layer model. *Icarus* **64,** 531–548 (1985).
8. Nicholson, P. *et al.* Saturns rings I: optical depth profiles from the 28 sgr occultation. *Icarus* **145,** 474–501 (2000).
9. Colwell, J. E., Esposito, L. W. & Bundy, D. Fragmentation rates of small satellites in the outer solar system. *J. Geophys. Res.* **105,** 17589–17600 (2000).
10. Esposito, L. W. & Colwell, J. E. Creation of the Uranus rings and dust bands. *Nature* **339,** 605–607 (1989).
11. Colwell, J. E. & Esposito, L. W. Origins of the rings of Uranus and Neptune. I. Statistics of satellite disruptions. *J. Geophys. Res.* **97,** 10227–10241 (1992).
12. Esposito, L. W. *et al.* Ultraviolet imaging spectroscopy shows an active saturnian system. *Science* **307,** 1251–1255 (2005).
13. Porco, C. C. *et al.* Cassini imaging science: initial results on Saturn's rings and small satellites. *Science* **307,** 1226–1236 (2005).
14. Dones, L., Cuzzi, J. N. & Showalter, M. R. Voyager photometry of Saturn's A ring. *Icarus* **105,** 184–215 (1993).
15. Colwell, J. E., Esposito, L. W. & Sremčević, M. Self-gravity wakes in Saturn's A ring measured by stellar occultations from Cassini. *Geophys. Res. Lett.* **33,** 7201–7204 (2006).
16. Hedman, M. M. *et al.* Self-gravity wake structures in Saturn's A ring revealed by Cassini VIMS. *Astron. J.* **133,** 2624–2629 (2007).
17. Salo, H., Karjalainen, R. & French, R. G. Photometric modeling of Saturn's rings. II. Azimuthal asymmetry in reflected and transmitted light. *Icarus* **170,** 70–90 (2004).
18. Weidenschilling, S. J., Chapman, C. R., Davis, D. R. & Greenberg, R. in *Planetary Rings* (eds Greenberg, R. & Brahic, A.) 367–415 (Univ. Arizona Press, Tucson, 1984).
19. Albers, N. & Spahn, F. The influence of particle adhesion on the stability of agglomerates in Saturn's rings. *Icarus* **181,** 292–301 (2006).
20. Showalter, M. R., Cuzzi, J. N., Marouf, E. A. & Esposito, L. W. Satellite 'wakes' and the orbit of the Encke Gap moonlet. *Icarus* **66,** 297–323 (1986).
21. Showalter, M. R. Visual detection of 1981S13, Saturn's eighteenth satellite, and its role in the Encke gap. *Nature* **351,** 709–713 (1991).
22. Seiß, M., Spahn, F., Sremčević, M. & Salo, H. Structures induced by small moonlets in Saturn's rings: implications for the Cassini Mission. *Geophys. Res. Lett.* **32,** 11205–11208 (2005).
23. Lewis, M. C. & Stewart, G. R. Features around embedded moonlets in Saturn's rings: the role of self-gravity and particle size distributions. *Icarus* (submitted).
24. Durda, D. D. *et al.* Size frequency distributions of fragments from SPH/N-body simulations of asteroid impacts: comparison with observed asteroid families. *Icarus* **186,** 498–516 (2007).
25. Karjalainen, R. & Salo, H. Gravitational accretion of particles in Saturn's rings. *Icarus* **172,** 328–348 (2004).
26. Hedman, M. M. *et al.* Saturn's dynamic D ring. *Icarus* **188,** 89–107 (2007).
27. Michel, P., Benz, W. & Richardson, D. C. Disruption of fragmented parent bodies as the origin of asteroid families. *Nature* **421,** 608–611 (2003).
28. Daisaka, H., Tanaka, H. & Ida, S. Viscosity in a dense planetary ring with self-gravitating particles. *Icarus* **154,** 296–312 (2001).
29. Cuzzi, J. N. & Estrada, P. R. Compositional evolution of Saturn's rings due to meteoroid bombardment. *Icarus* **132,** 1–35 (1998).
30. Spahn, F. & Sponholz, H. Existence of moonlets in Saturn's rings inferred from the optical depth profile. *Nature* **339,** 607–608 (1989).
31. Tiscareno, M. S., Burns, J. A., Hedman, M. M. & Porco, C. C. The population of propellers in Saturn's A ring. *Astron. J.* (submitted).

Supplementary Information is linked to the online version of the paper at www.nature.com/nature.

Acknowledgements We acknowledge the efforts of the Cassini ISS team in the design and operation of the ISS instrument. This work was supported by the Cassini project, Deutsches Zentrum für Luft und Raumfahrt, Deutsche Forschungsgemeinschaft and the Academy of Finland.

Author Information Reprints and permissions information is available at www.nature.com/reprints. Correspondence and requests for materials should be addressed to M.S. (miodrag.sremcevic@lasp.colorado.edu).